Journal of The Electrochemical Society, **154** (1) C60-C66 (2007)
0013-4651/2006/154(1)/C60/7/$20.00 © The Electrochemical Society

Fabrication and Characterization of Porous Anodic Alumina Films from Impure Aluminum Foils

Daniel Lo and R. Arief Budiman[z]

Department of Mechanical and Manufacturing Engineering, University of Calgary, Calgary, Alberta, Canada T2N 1N4

We report here on the fabrication of porous anodic alumina (PAA) films from commercially available impure aluminum foil. While the expensive ultrapure PAA films are restricted to potential applications in nanoelectrophotonics, the impure PAA films are more suitable for large-scale applications, such as in catalysis and filtration. The anodization current behavior and chemical composition of the resulting PAA films from impure and ultrapure foils were found to be similar for the same set of anodizing conditions. However, the PAA films from impure aluminum foil contained pore arrays of much smaller size and less consistently sized pores than those of PAA from ultrapure foils. We find that these qualities are improved by either annealing or electropolishing the aluminum foil prior to anodization, although not to the degree of PAA produced from ultrapure foils. Greater improvement is found for annealed foils compared to electropolished foils.
 [DOI: 10.1149/1.2387104]

Manuscript received August 2, 2006. Available electronically December 1, 2006.

Porous anodic alumina (PAA) has been actively studied over the past 50 years[1-3] due to its appearance in metal finishing applications and its unique morphology. PAA is produced by electrochemical anodization of aluminum in an acidic electrolyte, with the PAA forming as a product on the surface of the aluminum. The structure of PAA consists of a barrier layer of alumina, upon which a layer of porous alumina appears. The pores produced are usually irregular in shape and distributed randomly about the surface. However, the pores can, under specific anodization conditions, become circular in shape, with consistent diameter, and become arranged in a hexagonal close-packed array. This self-organized PAA can occur with no manipulation of the morphology of the aluminum prior to anodization. In this case, ordered pore domains can reach sizes of a few micrometers, when ultrapure (99.99% or greater) aluminum is used, with rotational defects in the hexagonal array appearing between adjacent domains.

In recent years, PAA has generated interest as a candidate material for nanotechnology applications. The pore diameter, pore spacing, and film thickness are all controllable through the anodization conditions, such as the choice of electrolyte, temperature, and anodization time.[4-7] The pore spacing may also be controlled through postanodization techniques such as chemical etching.[8] As well, the size of ordered pore domains can be increased through treatment of the aluminum prior to anodization. These treatments may involve smoothing the aluminum with mechanical or electrochemical polishing[9] or may pattern the aluminum in order to encourage pore formation at specific sites, whereupon the pore array is no longer self-organized. Such patterning may be done through nanoindentation,[8,10] electron beam lithography, or deposition of aluminum onto a textured surface.[11] This controllability of the pore morphology has led to investigation and application of PAA as a template for microsystem structures[6] and nanomaterial growth, such as nanowires[12-15] and carbon nanotubes.[16] Also PAA has been proposed as a medium for molecular filtration and catalysis.[17]

The production methods for PAA as explained in these investigations and applications suffer from several drawbacks, however. The aluminum foil or plate usually used in anodization is ultrapure in grade, which is very expensive, limiting the use of PAA in many cases.[18] Use of lower purity aluminum alloys in these areas does not appear to be well-studied in the case of those applications listed above. It is suggested that anodizing impure aluminum alloy results in disordered pore arrangement.[18] The use of patterning, either through electron-beam lithography or nanoindentation, could improve these reported results, but these methods are also expensive, time-consuming, and have limited production rates. Other reported pretreatment methods, such as ultrasonic cleaning, polishing, and annealing, further consume time and reduce production rates.[19,20] As well, many of the procedures produce very thin PAA films. The motivation here appears to be the production of PAA films for nanoelectrophotonic applications. These thin films are difficult to handle and process on the macroscopic scale, which may limit large-scale application in catalysts and filtration.

In this study, we investigate the use of commercially available aluminum alloy in production of PAA as a cost-reducing measure. In addition, the production of films thick enough for easy manual handling is investigated. The consistency of pore size and degree of pore ordering on the resulting PAA is compared to PAA produced from ultrapure aluminum. Comparisons of the chemical composition and current behavior for PAA films anodized from ultrapure and impure aluminum foils are also made to highlight any differences in their formation.

Experimental

PAA was produced through anodization of both ultrapure and impure aluminum foils, using a two-step anodization process. Ultrapure foils (Goodfellow, 99.99% Al, annealed, 0.09 mm thickness) were cut into 5×5 mm samples and mounted onto glass slides. The samples were then anodized for 18 h in 0.3 M oxalic acid at a constant voltage of 40 V vs a copper cathode, with the temperature maintained at 7 ± 2°C. The resulting oxide layer was then etched away in an 0.5 M phosphoric/0.2 M chromic acid mixture at 80°C for 1 h. The samples were then anodized again in the previously used electrolyte under the same conditions for 15 min. Afterwards, the samples were removed from the glass slide and floated on saturated mercury(II) chloride solution until the underlying aluminum was removed from the alumina film. Some of the resulting PAA films were treated in 5% w/w phosphoric acid to remove the barrier layer and widen the pores, while others were left as is after the mercury(II) chloride treatment.

Production of PAA using impure aluminum alloy followed a similar method. The foils (Alcan heavy duty aluminum foil) were cut into 35 mm diam disks. At this point, some samples were annealed in nitrogen at 600°C for 1 h, while others were left in their as-rolled state. The resulting foils were then sealed about a glass tube and anodized for 1 h in the same conditions as the ultrapure aluminum samples (0.3 M oxalic acid, 40 V, 7 ± 2°C). The oxide layer was then removed using the same etch solution (0.5 M phosphoric/0.2 M chromic acid, 80°C) for 4 min. The resulting aluminum was then anodized in the same electrolyte previously used under the same conditions for 4 h. For all anodizations, the electrical current was recorded, with a sampling rate of 2 samples/s. As well, the conductivity and pH of the electrolyte was taken before the first anodization, between the anodizations, and after the second

[z] E-mail: rbudiman@ucalgary.ca

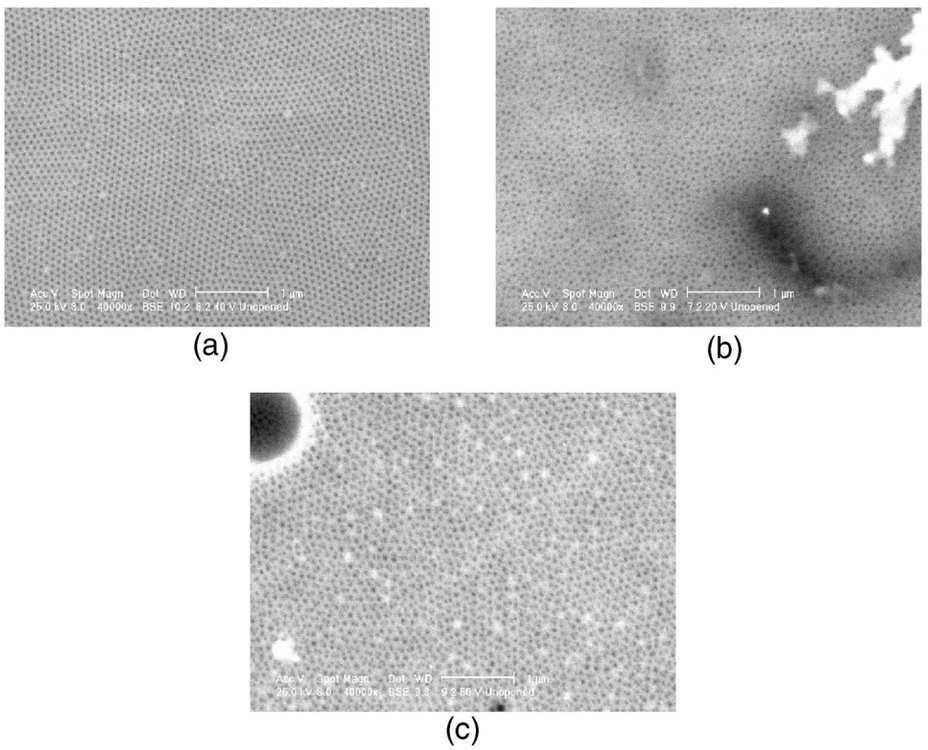

Figure 1. SEM micrographs (backscatter) of top surface of PAA films from anodized ultrapure aluminum foil in 0.3 M oxalic acid with 15 min second anodization. The anodization voltages were (a) 40, (b) 20, and (c) 56 V, relative to copper cathode. Optimal pore ordering and uniformity in shape are achieved at 40 V, matching results achieved elsewhere. At the other voltages, the pores lose their hexagonal ordering and become less consistent in shape.

anodization. Some samples (annealed and not annealed) were then given a heat-treatment in atmosphere at 600°C for 1 h, as described by Chen et al.,[18] while others (annealed and not annealed) were left as is. Afterwards, all samples were given the aluminum removal treatment [saturated mercury(II) chloride solution, room temperature].

The effect of electropolishing on the pores of the PAA was also investigated. A series of PAA was produced from impure aluminum foils as before, with electropolishing performed on some of these samples prior to the first anodization. Electropolishing of the foils was performed in an aqueous solution of 40% w/w phosphoric acid and 40% w/w sulfuric acid at 15 V potential (relative to a copper cathode) and 60°C temperature for 1 min. Four samples were created for this set: the first was given annealing, with the same procedure as before, the second was given the electropolishing treatment, the third was given both treatments, and the final sample was left in its as-rolled state.

Characterization of the morphology of all resulting PAA films was done using scanning electron microscopy (SEM, Philips XL30) after the samples were made conductive through either carbon evaporation or gold sputtering. In addition, X-ray photoelectron spectroscopy (XPS, Kratos Axis Ultra spectrometer) was performed on the PAA films and the impure aluminum foil to determine their chemical compositions. Aluminum foils from the electropolish set of samples were analyzed with atomic force microscopy (AFM, JPK NanoWizard) to determine surface roughness.

Results and Discussion

SEM images.— PAA samples were characterized using SEM, with particular attention to the morphology of their top and cross-sectional surfaces. Figure 1a shows a micrograph of the top surface of a PAA film produced from ultrapure aluminum foil under an anodization voltage of 40 V. The resulting pores are fairly uniform in shape and diameter, with a diameter of about 50 nm. The pores are also arranged in a hexagonal array, with an interpore spacing of about 100 nm and an ordered domain size of 1.1 μm. The ordered hexagonal domains of pores are separated by rotational defects, where pores have either five or seven nearest neighboring pores instead of the expected six. The resulting domains have their hexagonal array orientation rotated relative to neighboring ordered domains.

Further anodizations with ultrapure aluminum indicate an optimal voltage exists for anodization in oxalic acid. Figure 1b and c shows PAA films produced under identical conditions as that shown in Fig. 1a, except that the anodization voltages were 20 and 56 V, respectively. In these cases, the ordered hexagonal domains no longer appear, with pores appearing at random locations and with inconstant diameter. The pore diameter varies between about 30 and 50 nm in the 20 V sample, while the diameter varies between about 30 and 60 nm in the 56 V sample. The smaller pores appear to have smaller interpore distances than the larger pores in the 56 V sample, while pores in the 20 V sample appear more evenly distributed. This optimal voltage of 40 V for pore ordering matches observations reported elsewhere for oxalic acid electrolytes.[4,21,22]

The experimental method for producing PAA films from ultrapure aluminum resulted in very thin samples due to the short second anodization time used. As a result, these films were very fragile and brittle, causing problems with handling both inside solutions and when dry. PAA films of this order of thickness are likely usable in the manufacture of nanomaterials.[16] However, the fragility of such samples is likely to limit use in macroscopic applications, such as filtration and catalysis. Reported growth rates for PAA in stirred oxalic acid at 40 V range between 40 and 130 nm/min,[14,16] indicating that our PAA has a likely thickness between 600 and 1950 nm. Because our PAA was produced in unstirred electrolyte, the growth rate is expected to be towards the lower end of this range, because transport and reaction of the ion reactants would be reduced by the lack of forced convection.

The PAA films produced from the impure aluminum foil appeared different from the ultrapure-derived films under SEM characterization. Figure 2a and b shows SEM micrographs of PAA derived from as-rolled impure aluminum given no heat-treatment and the heat-treatment described by Chen et al.,[18] respectively. In both these cases, the pores appear to have no planar ordering and are of

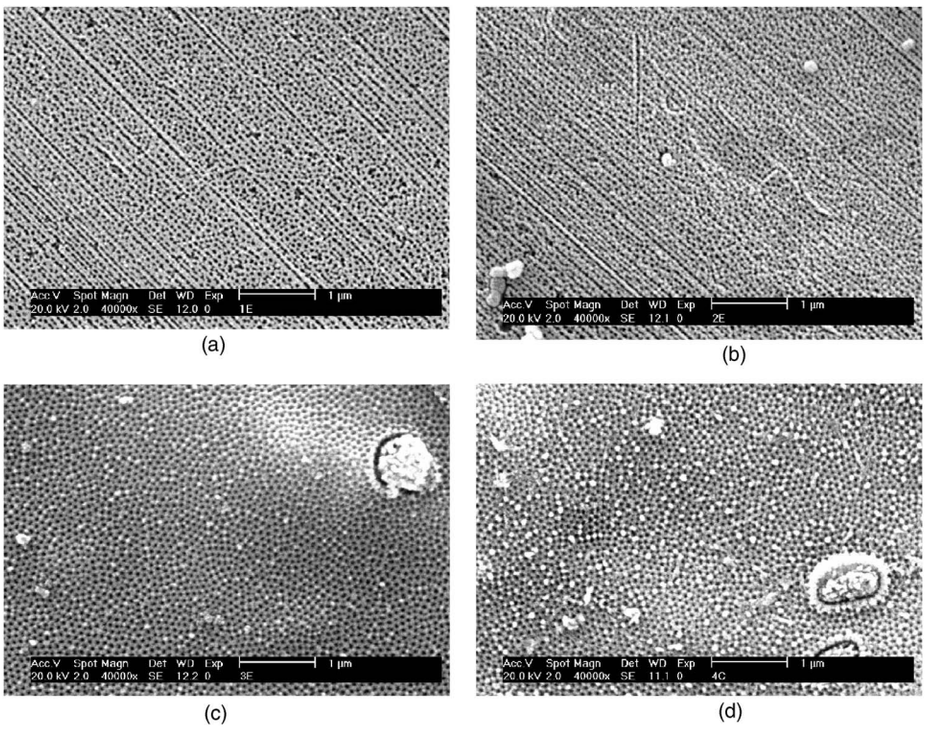

Figure 2. SEM micrographs (secondary) of PAA from anodized impure aluminum foil in 0.3 M oxalic acid with 4 h second anodization. Each sample was either given (a) no treatments, (b) oxide heat-treatment, (c) foil annealing, or (d) foil annealing and oxide heat-treatment. Annealing of the foils prior to anodization appears to improve pore ordering and geometric consistency, while heat-treatment appears to have no effect.

inconstant, noncircular shape. The pores vary in size from about 25 to 60 nm in width, with many pores appearing merged with neighboring pores. Lines of pores, with parallel spacing ranging from about 60 to 120 nm, do appear at some locations on the alumina. However, the pores are not evenly spaced along these lines and are, in most cases, merged with neighboring pores. In addition, many pores appear at random between these lines. The lines appear to follow the direction of rolling in the aluminum foil from which the alumina was derived.

Figure 2c and d shows PAA from impure aluminum foils that were annealed prior to anodization and given no heat-treatment and heat-treatment, respectively. In these cases, the pore diameter was more consistent; most pores were about 50 nm in diameter, although some pores appeared as small as about 30 nm. The interpore distance appears fairly consistent at about 80 nm. However, hexagonal ordered domains in these samples are small and tend to span only a few pores. Other areas of similar size appear to have consistent pore spacing but no hexagonal ordering. In relation to the expected hexagonal array, it may be said that the pore array contains a large amount of rotational defects.

The similarity in surface structure between samples that were given no heat-treatment and heat-treatment indicates that we were unable to reproduce the improved pore ordering reported by Chen et al.[18] through heat-treatment. Instead, it appears annealing of the foils prior to anodization results in a slight improvement on the ordering of the pores. It is reported elsewhere that minimal surface roughness is needed for ordered pore formation, achieved mostly through electrochemical polishing.[9,23] As well, it is suggested that grain boundaries have differing oxidation characteristics than the crystalline aluminum within a single grain, which would yield an uneven etching front and a disordered pore arrangement.[23] The results achieved here would agree with these proposed mechanisms, because annealing would result in a smoother surface and reduce the amount of grain boundaries present.

The heat-treatment procedure also introduced further difficulties in handling the resulting PAA films. Upon removal from the furnace, the samples had a tendency to curl about themselves, with the aluminum foil curling along the outside and encompassing the curled alumina on the inside. The curling is likely due to the differing coefficients of thermal expansion of the aluminum and alumina, resulting in different rates of contraction for each layer upon removal from the furnace. The resulting curled samples, of about 5 mm diam, could not be straightened out without fracturing the alumina layer. As a result, flat samples of comparable size to the original aluminum foil (35 mm diam) could not be created. Instead, samples of only a few millimeters width, of sufficient flatness for SEM characterization, were recovered from these samples. As well, the aluminum removal treatment was found to take significantly longer for heat-treated samples than samples given no heat-treatment. We believe the formation of oxide on the back surface of the aluminum foil during the heat-treatment, which would shield the aluminum metal from the mercury(II) chloride solution, is responsible for this increased treatment time.

In general, the use of mercury-based solutions limits application of through-pore PAA films due to the prior's toxicity. The above results indicate that mercury(II) chloride is also sensitive to oxide formation on the foil and is be effective in aluminum removal unless the back side of the aluminum is largely oxide free. Other aluminum-removal solutions have been proposed as more environmentally friendly and safer alternatives, such as copper(II) sulfate in hydrochloric acid[16] or copper(II) chloride in hydrochloric acid.[19] In addition, the greater solubility of aluminum oxide in these acidic solutions would likely reduce the chance of excess surface oxide thwarting the oxide removal treatment. However, this acidity may also affect the PAA grown on the other side, causing possible etching and pore widening. Thus, these considerations are likely needed in the case of using these aluminum removal solutions to produce through-hole PAA.

The SEM micrographs appeared to show surface contamination of some kind on several of the specimens, appearing as bright points or areas obscuring the porous structure of the PAA. This may be caused by mercury(II) chloride crystallizing on the surface during aluminum removal treatment, as it initially appeared to be more prevalent in samples that were immersed in the solution longer. However, the appearance of these surface features was not consistent, and they were still found in cases where no mercury(II) chlo-

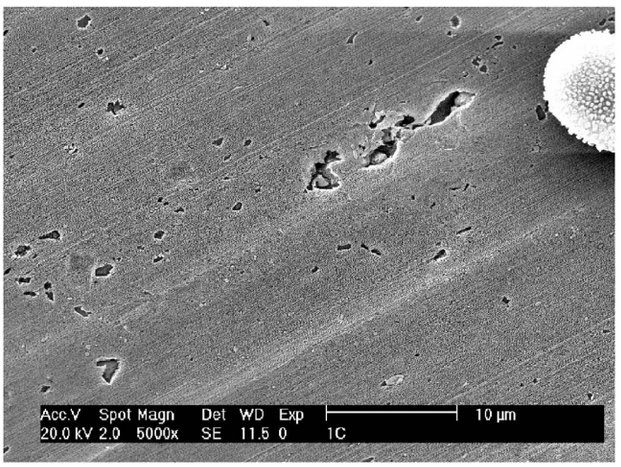

Figure 3. SEM micrograph of top surface of PAA film from impure aluminum foil. Large holes, of micrometer size, are visible on this sample. These features could limit applications of PAA where consistent and limited pore size is necessary.

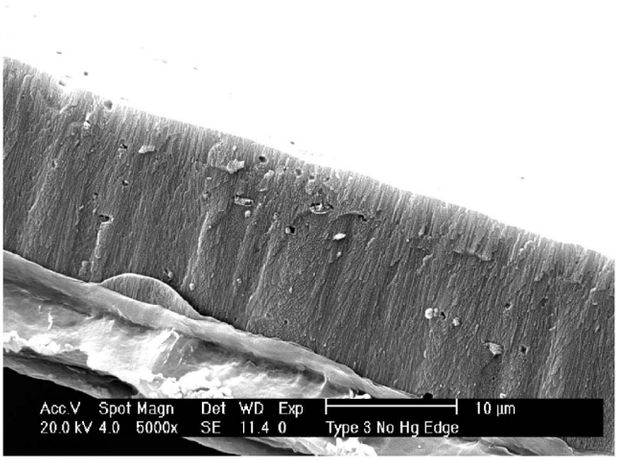

Figure 4. SEM micrograph of cross section of a PAA film still attached to its underlying impure aluminum foil. The thickness of the PAA is estimated to be 12–15 μm, corresponding to an oxide growth rate of 50–63 nm/min. This value is similar to those reported for ultrapure aluminum.

ride was applied (see below, Fig. 6a). Other possible sources of this surface contamination may include the gold coating used for SEM visualization and residues from the electrolyte or organic solvents used. However, the precise origin of these features requires further investigation.

The SEM micrographs also revealed additional surface features aside from the expected pore arrays. Several locations on the samples contained apparent holes much larger than the pores, with these holes appearing not to be through-thickness and having additional features at their bottoms. Figure 3 shows such holes on a PAA film anodized from impure aluminum (the same sample as in Fig. 2a). While the pores are about 25–60 nm in width, the larger holes range from 200 nm to 2.6 μm in width and are irregular in shape. Such features did not appear on micrographs of PAA films produced from ultrapure aluminum. Whatever their cause, such features cause limitations in the applications of these films in, for example, large-scale masking and filtration uses, as they are of vastly greater size than that of the pores and introduce large deviations from the expected morphological properties.

The PAA films produced from impure aluminum and shown in Fig. 2 were given an anodization of 4 h, as opposed to the 15 min anodization given to the ultrapure aluminum foils. As a result, the PAA from impure aluminum were much thicker and could withstand manual handling without fracturing or shattering, as was the case with the thinner films from ultrapure aluminum. A SEM micrograph of the cross section of one of these films, still attached to the aluminum foil, is shown in Fig. 4. From this, the film thickness is estimated to be between 12 and 15 μm, which corresponds to a growth rate from about 40 to 60 nm/min. Thus, the growth rate is similar to those reported for PAA from ultrapure aluminum.

Other micrographs taken from the same cross section indicate the presence of pores throughout the thickness of the PAA. Figure 5 shows a micrograph of the cross section of a PAA film anodized from an impure, annealed aluminum foil. Parallel striations of about 50 nm width and 100 nm parallel spacing appear in this view. These dimensions correspond to the pore diameter and spacing found in the micrographs of the top surface of the PAA formed under the same conditions (Fig. 2c). Although these structures appear throughout the cross section of the film, it is unclear if individual pores are contiguous through the entire thickness of the PAA, due to the uneven fracturing of the film and exposure of pores at different depths in the cross section. The uneven fracture is likely a result of the low ordering of the pores, because a PAA film with ordered pores would be expected to fracture perfectly along straight lines of pores.[23]

Electropolishing was found to have an effect on the ordering and spacing of the pores produced upon anodization, relative to pores produced from as rolled aluminum foil. AFM characterization of a 10×10 μm square of the foils prior to anodization indicate a surface roughness (standard deviation of elevation) of 28.8 nm for the electropolished foil and 39.4 nm for the electropolished and annealed foil. Figure 6a shows PAA produced from an electropolished impure aluminum foil with no annealing treatment. The pores in this case assume a fairly uniform circular shape and a uniform spacing, with most diameters ranging from 50 to 70 nm and an interpore distance of 85–105 nm. In addition, pores of smaller diameter, about 35 nm, appear randomly interspersed with the more uniform-diameter pores. As before, the pores appear to form hexagonal domains with each other but only over short distances and with considerable disorder outside of these domains. The hexagonal domains do not appear to exceed 400 nm in width in this case and thus include only a few pores each time.

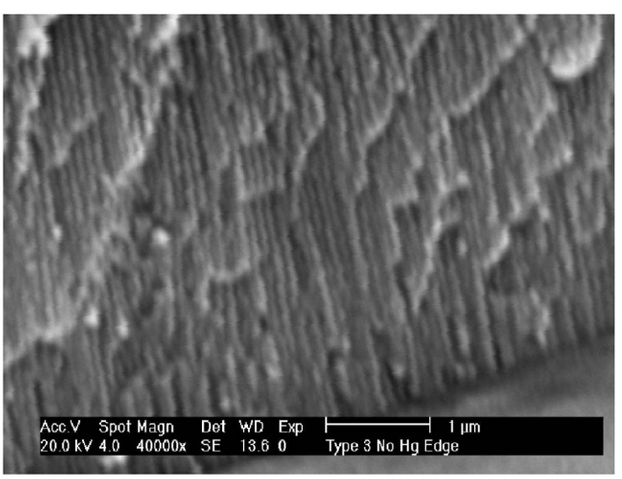

Figure 5. SEM micrograph of cross section of a PAA film from impure aluminum foil. The corrugated features visible correspond to pores, due to their similar dimensions. The disordered arrangement of the pores prevents a clean fracture from forming, resulting in layers of pores appearing in front of others.

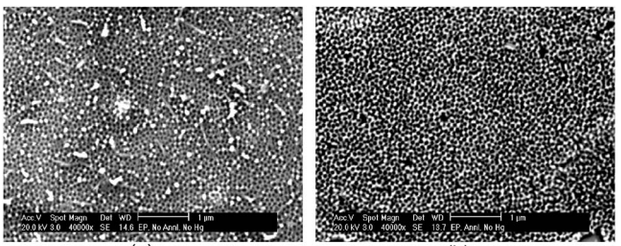

Figure 6. SEM micrographs of top surfaces of PAA anodized from (a) electropolished and (b) electropolished and annealed impure aluminum foil. The results for electropolished aluminum are similar to those for annealed aluminum, with pores assuming consistent diameter and small-scale hexagonal ordered domains. When annealed and electropolished, the foil produces PAA with merged pores, which appear to destroy any hexagonal ordering.

Figure 6b shows a PAA film produced from an impure foil that was given both the electropolishing and annealing treatments. In this case, many of the pores were found merged with adjacent pores, destroying the hexagonal array found earlier. Some unmerged pores were still visible in this case, with these pores having a diameter of about 65–85 nm and a spacing of 85–105 nm. In addition, some of these pores do appear to be arranged in small hexagonal domains, indicating that the same mechanism of self-organization exists but is disrupted by pores growing large enough to merge with neighboring pores.

The improved pore ordering observed on the PAA derived from electropolished aluminum indicates that the surface roughness of the source aluminum affects the formation and distribution of pores, with reduced surface roughness resulting in improved pore ordering.[9] In this instance, the surface roughness was reduced to a value on the order of the pore diameter, although this value was greater than that reported elsewhere.[6,9] As well, the electropolishing treatment is expected to even the distribution of rough features about the foil, in comparison to those found in as-rolled foil. In that instance (Fig. 2a), the roughness features are expected to align with the rolling direction, which appeared to force the pores to appear in that direction. With the electropolishing treatment, the roughness may no longer influence pore formation greatly, due to the even distribution of surface features.

The improvement of pore ordering on the PAA from electropolished foil is comparable to that of PAA from annealed foil. Because annealing is expected to induce grain growth and increase distances between grain boundaries, and thus reduce surface roughness, the mechanism may be the same in this case as in the electropolished case. However, applying both annealing and electropolishing treatments to the aluminum appears to destroy the pores in the resulting PAA. It appears the mechanism of destruction here is through the growth of larger pores, as the interpore spacing is similar between the electropolished and annealed-and-electropolished cases while the pore diameters appear larger in the latter case. However, this phenomenon is not found in other cases,[6] possibly indicating that the purity of the foil has a effect on electropolishing results. The precise mechanism of the array destruction here requires further investigation.

Table I. Percent atomic concentrations of impure aluminum foil as-received and after 30 min ion beam etch.

	Al	O	C	N	Fe	Mg	Ca
As-received	30.30	48.70	18.14	0.86	–	1.74	0.25
After 30 min etch	93.76	4.06	1.18	3.16	0.71	–	–

XPS analysis.— Analysis was performed on the surface of the aluminum foil and at a point within the foil. The interior analysis was performed by sputtering the foil with 4 keV argon ions for 30 min.

The XPS results are summarized in Table I. The large concentrations of carbon and oxygen at the surface are likely attributable to atmospheric contamination and the presence of a naturally formed oxide layer at the surface. Within the metal (i.e., after a period of electron etching), the concentration of carbon and oxygen drop significantly. Because the carbon concentration is very low within the metal (0.54% by mass), it is presumed that this, along with detected oxygen and nitrogen, originated in the atmosphere and was incorporated during manufacturing of the foil.

As a result, the impure aluminum foil is still largely aluminum, with a mass concentration of 93.78%. The only alloying element remaining in the foil is iron, with a mass concentration of 1.52%. If the atmospheric components are neglected, this translates into mass concentrations of aluminum and carbon of about 98.4 and 1.6%, respectively. From this and the SEM micrographs of the resulting PAA films, it appears even small amounts of alloying impurities in the aluminum foil can greatly affect the degree of pore ordering in the resulting PAA. The correlation or mechanism linking aluminum foil impurities and the pore ordering in the resulting PAA require further investigation. Stress models have previously been proposed as mechanisms for pore formation and ordering.[4,6] Our results suggest a more dominant role of the impurities. In addition, pore ordering in PAA has been found to be affected by applied stresses on the aluminum foil from which they were formed.[24] It is possible the alloying atoms introduce localized stresses, which affect the location of pore formation and resulting pore ordering.

XPS analysis was performed on the PAA films while being sputter etched with argon ions at 4 keV over an area of 1.5×1.5 mm. Results were obtained during the etching process, allowing for chemical compositions throughout the thickness of the PAA film to be determined.

The chemical composition of a typical PAA film from ultrapure aluminum is presented in Fig. 7a. In all tested samples, the ratio of atomic concentrations between aluminum and oxygen is approximately 2:3 at all etch times. It is thus concluded that the film is composed of aluminum oxide throughout, while no other possible products, such as aluminum hydroxide,[25] are present.

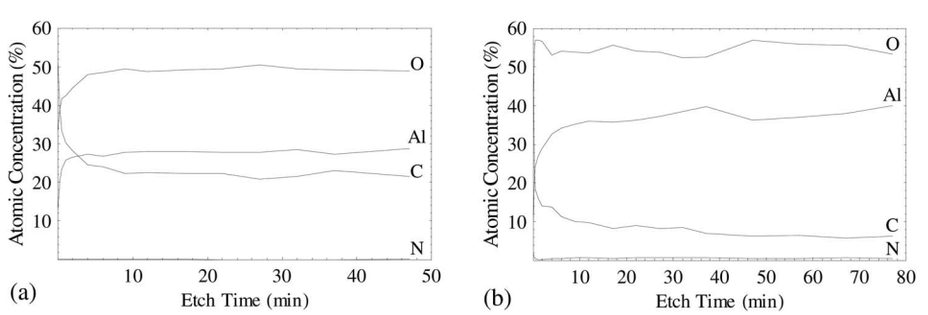

Figure 7. XPS results for PAA film anodized from (a) ultrapure aluminum and (b) impure aluminum foils. The chemical profiles are similar for both PAA films. The persistence of carbon in the PAA film is attributed to anion (oxalate) incorporation into the film.

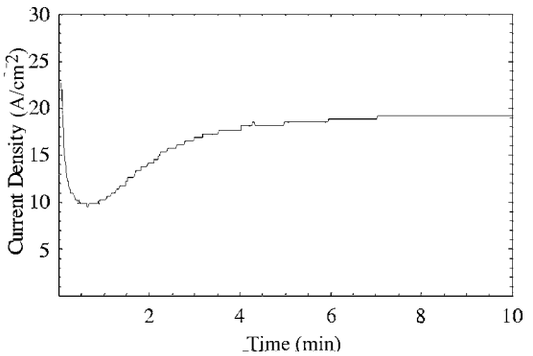

Figure 8. Plot of current density vs time for second anodization of ultrapure aluminum foil. The characteristic minimum and steady-state current behaviors for PAA are visible.

Detection of nitrogen and carbon was also performed. In both cases, the atomic concentration decreases greatly when moving from the surface into the interior of the alumina (i.e., with greater etch time). As in the case of the impure aluminum foil, the source of heightened carbon and nitrogen concentrations at the surface may be due to atmospheric contamination. In addition, organic solvents, such as methanol, were used to rinse samples, which may have contributed additional carbon to the surface. The concentration of nitrogen, although noticeably greater at the surface, did not exceed 2% at any time during the XPS analysis, and the production procedure for ultrapure aluminum involved no nitrogen compounds.

The atomic concentration of carbon, on the other hand, remained at higher levels within the PAA film, ranging from 10 to 40% among all samples after the initial drop in concentration. Moreover, the concentration of carbon appears to be decreasing slightly in all samples at greater depths in the PAA films. In this case, the carbon may originate from oxalate ions incorporated into the alumina during anodization, matching observations made elsewhere.[14,26] In addition, this would explain the slight decrease of carbon concentration with increasing depth. Because anion incorporation is driven by diffusion, transport of oxalate anions becomes more difficult through longer pores, resulting in lower concentrations at greater depths. This is also indicated by the slowly decreasing current observed during later stages of the anodizations.

XPS results for PAA anodized from impure aluminum are given in Fig. 7b. The chemical composition is found to be similar to that for the PAA derived from pure aluminum. As was described earlier, the impure aluminum foil is still largely composed of aluminum. The small amount of impurities present do not appear to affect the chemical composition of the PAA film, indicating little interference by them with the formation of oxide or the incorporation of electrolyte anions into the oxide. The SEM micrographs indicate that impurities may have an effect on the porous morphology of the PAA film. In keeping with the oxide stress model, the impurity atoms present in the foil are likely lost to the electrolyte, as opposed to being incorporated into the alumina layer. The resulting vacancies in the aluminum may cause uneven formation of the alumina during anodization, resulting in uneven stresses at the metal/oxide interface and affecting pore formation in the oxide. This would result in impurities affecting pore ordering without necessarily being found in the oxide layer itself.

Electrical current.— The electrical current passing through the apparatus was measured throughout the second anodization of the ultrapure samples. A typical current–time plot for this case is shown in Fig. 8. The current pattern, with a rapidly decreasing and pronounced minimum current, followed by a larger steady-state current, matches the typical current behavior reported elsewhere.[5,20,23,25] In this case, the minimum current was found to be about 9.4 A/m^2, while the steady-state current was about 19.2 A/m^2.

It is believed the initially high current followed by its rapid descent is the result of the barrier layer formation,[19,23] followed by pore nucleation and growth at the minimum current.[25] The steady-state current is caused by the oxide growth rate at the metal/oxide interface and the oxide etch rate at the solution/oxide interface at the pore bottoms being equal.[19,23] The pores do not begin to form by etching of the oxide until after an oxide barrier layer is built up, upon which resistive heating[19] and weakening of electrostatic repulsion[25] initiate etching of the oxide layer.

The current behavior for the impure aluminum foils appears similar to those for the ultrapure aluminum foils presented above. For the case of the first anodization, shown in Fig. 9a, the average minimum current over all annealing and heat-treatment conditions is 21.5 A/m^2 and the average steady-state current is 22.4 A/m^2. However, the current behavior for times before steady-state is reached is slightly different in the second anodization cases. As shown in Fig. 9b, the annealed samples reach a minimum current prior to anodization, while the nonannealed samples have no obvious minimum current at the start of the anodization, similar to the case of the thin films.

With the much longer second anodization, a steady-state current is not shown in the current–time plots. It is expected that with the long anodization, the growth of the oxide produces pores with increasing depth and aspect ratio. As a result, diffusion of ions, and thus current, slowly decreases. Because reactants for both oxide formation and dissolution must be transported down the pores, the growth and etch rates are expected to be affected by similar amounts, which would maintain even but decreasing pore wall growth.

This decrease in current after reaching the presumed steady-state current is observed in Fig. 10. The lack of stirring would further reduce the rate of ion transport, resulting in a still lower current than expected,[23] although this did not preclude ordered pore formation. In addition, a sinusoidal behavior is superimposed on the continuously decreasing current at later anodization times. Because this behavior does not cause sudden jumps in current, it appears not to be caused by hydrogen bubbles collecting on the foil. The oscillation suggests differences in the oxide formation and etching rates, which

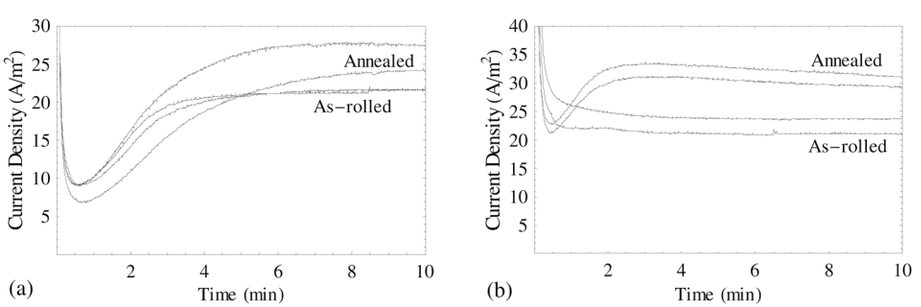

Figure 9. Plots of current density vs time over the first 10 min of the (a) first and (b) second anodizations of impure aluminum foils. The current behaviors of the samples given no annealing and annealing are similar.

Table II. Conductivity and pH values of electrolyte during anodization of impure foils.

	Before first anodization		After first anodization		After second anodization	
Sample	Conductivity (mS/cm)	pH	Conductivity (mS/cm)	pH	Conductivity (mS/cm)	pH
No treatments	91.1	0.731	92.0	0.770	96.9	0.723
Heat treated	90.7	0.793	91.7	0.782	92.0	0.788
Annealed	90.9	0.757	91.9	0.760	93.7	0.739
Annealed, heat treated	99.5	0.747	98.8	0.737	101.8	0.742

would lead to an inconsistant barrier layer thickness and thus changes in the resistance of the PAA film. Further investigation of this effect is needed.

Changes are expected in the composition of the electrolyte, because some of the aluminum ions produced at the anode are released into the solution instead of being incorporated into the alumina.[4,25] However, conductivity and pH measurements indicate limited change in either value as a result of the anodizations. The slight increase in pH is attributed to loss of hydrogen ions to hydrogen gas evolution at the anode, while the changes in conductivity are attributable to the release of aluminum ions in solution. Table II summarizes the conductivity and pH values of the electrolyte at various points during PAA production.

Conclusions

We have demonstrated the production of porous anodic aluminum from the anodization of impure aluminum foils. The effect of annealing and electropolishing of the foils prior to anodization and the heat-treatment of samples after anodization were determined. In all cases, compared to PAA produced from ultrapure aluminum foils, the PAA produced from the impure foil has reduced pore ordering. For as-rolled impure foil, anodization produces PAA with noncircular pores partially arranged in parallel lines of pores, while annealed impure foil produces round pores within hexagonally ordered domains containing a few pores. No effect was seen between samples given heat-treatment and samples given no heat-treatment. As well, electropolishing the foils prior to anodization did improve pore consistency and ordering, although on a scale less than that for annealing, and applying both annealing and electropolishing treatments yielded a destroyed ordered pore structure. The growth rate, chemical composition, and current behavior of PAA films anodized from ultrapure and impure foils were similar, despite the differences in morphology. In addition, the impure aluminum was found to contain mostly aluminum, indicating a strong effect on pore ordering by impurity atoms. We conclude PAA films with some pore ordering are producible from lower cost impure aluminum foils. In addition, films thick enough to withstand manual handling have been produced from impure aluminum foil.

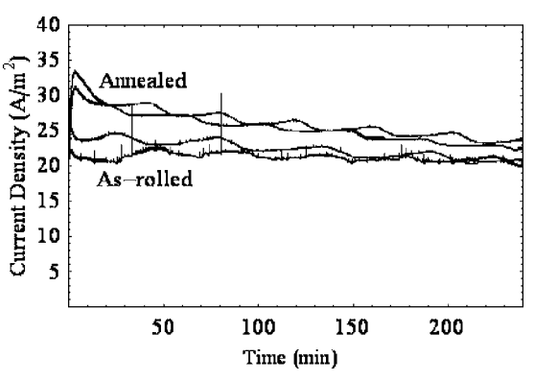

Figure 10. Plots of current density over the entire second anodization of impure aluminum foils. An oscillating current behavior appears to be superimposed on the steadily decreasing current.

Acknowledgments

We thank D. Kim, R. Humphrey, D. Karpuzov, and J. McNeely for technical assistance. This work was supported by the Natural Sciences and Engineering Research Council of Canada.

University of Calgary assisted in meeting the publication costs of this article.

References

1. F. Keller, M. S. Hunter, and D. L. Robinson, *J. Electrochem. Soc.*, **100**, 411 (1953).
2. J. P. O'Sullivan and G. C. Wood, *Proc. R. Soc. London, Ser. A*, **317**, 511 (1970).
3. J. W. Diggle, T. C. Downie, and C. W. Goulding, *Chem. Rev. (Washington, D.C.)*, **69**, 365 (1969).
4. O. Jessensky, F. Müller, and U. Gösele, *Appl. Phys. Lett.*, **72**, 1173 (1998).
5. L. Ba and W. S. Li, *J. Phys. D*, **33**, 2527 (2000).
6. A. P. Li, F. Müller, A. Birner, K. Nielsch, and U. Gösele, *J. Appl. Phys.*, **84**, 6023 (1998).
7. W. Y. Zhou, Y. B. Li, Z. Q. Liu, D. S. Tang, X. P. Zou, and G. Wang, *Chin. Phys.*, **10**, 218 (2001).
8. H. Masuda, H. Yamada, M. Satoh, H. Asoh, M. Nakao, and T. Tamamura, *Appl. Phys. Lett.*, **71**, 2770 (1997).
9. M. T. Wu, I. C. Leu, and M. H. Hon, *J. Vac. Sci. Technol. B*, **20**, 776 (2002).
10. H. Masuda, H. Asoh, M. Watanabe, K. Nishio, M. Nakao, and T. Tamamura, *Adv. Mater. (Weinheim, Ger.)*, **13**, 189 (2001).
11. Z. Sun and H. K. Kim, *Appl. Phys. Lett.*, **81**, 3458 (2002).
12. G. Q. Ding, M. J. Zheng, W. L. Xu, and W. Z. Shen, *Nanotechnology*, **16**, 1285 (2005).
13. G. Sauer, G. Brehm, S. Schneider, K. Nielsch, R. B. Wehrspohn, J. Choi, H. Hofmeister, and U. Gösele, *J. Appl. Phys.*, **91**, 3243 (2002).
14. N. J. Gerein and J. A. Haber, *J. Phys. Chem. B*, **109**, 17372 (2005).
15. D. J. Peña, J. K. N. Mbindyo, A. J. Carado, T. E. Mallouk, C. D. Keating, B. Razavi, and T. S. Mayer, *J. Phys. Chem. B*, **106**, 7458 (2002).
16. G. Q. Ding, M. J. Zheng, W. L. Xu, and W. Z. Shen, *Nanotechnology*, **16**, 1285 (2005).
17. W. S. Chae, S. J. Im, J. K. Lee, and Y. R. Kim, *Bull. Korean Chem. Soc.*, **26**, 409 (2005).
18. C. C. Chen, J. H. Chen, and C. G. Chao, *Jpn. J. Appl. Phys., Part 1*, **44**, 1529 (2005).
19. J. H. Yuan, F. Y. He, D. C. Sun, and X. H. Xia, *Chem. Mater.*, **16**, 1841 (2004).
20. Y. Zhao, M. Chen, Y. Zhang, T. Xu, and W. Liu, *Mater. Lett.*, **59**, 40 (2005).
21. K. Nielsch, J. Choi, K. Schwirn, R. B. Wehrspohn, and U. Gösele, *Nano Lett.*, **2**, 677 (2002).
22. H. Masuda and K. Fukuda, *Science*, **268**, 1466 (1995).
23. O. Jessensky, F. Müller, and U. Gösele, *J. Electrochem. Soc.*, **145**, 3735 (1998).
24. G. D. Sulka, S. Stroobants, V. V. Moshchalkov, G. Borghs, and J.-P. Celis, *J. Electrochem. Soc.*, **151**, B260 (2004).
25. A. Despić and V. P. Parkhutik, in *Modern Aspects of Electrochemistry*, J. O'M. Bockris, R. E. White, and B. E. Conway, Editors, No. 20, p. 401 Plenum Press, New York, (1989).
26. G. C. Wood, P. Skeldon, G. E. Thompson, and K. Shimizu, *J. Electrochem. Soc.*, **143**, 74 (1996).